Journal of the Meteorological Society of Japan, Vol. 91, No. 5, pp. 639–653, 2013 **639**
DOI:10.2151/jmsj.2013-506

Impact of SST on Precipitation and Snowfall on the Sea of Japan Side in the Winter Monsoon Season: Timescale Dependency

Hiroshi G. TAKAHASHI

Graduate School of Urban Environmental Sciences, Tokyo Metropolitan University, Japan
Japan Agency for Marine-Earth Science and Technology, Yokohama, Japan

and

Takafumi IDENAGA

Graduate School of Urban Environmental Sciences, Tokyo Metropolitan University, Tokyo, Japan

(Manuscript received 7 November 2012, in final form 20 June 2013)

Abstract

We investigated the impact of the sea surface temperature (SST) over the Sea of Japan on precipitation and snowfall on the Sea of Japan side of Honshu, Japan, using precipitation and snowfall data from Automated Meteorological Data Acquisition System (AMeDAS) stations, records of sea level pressure from meteorological stations, wind fields from the Japanese 25-year reanalysis (JRA25) dataset, and multiple SST datasets. We examined the data on various timescales from daily to monthly because SST over the Sea of Japan also varies on timescales shorter than a month.

The results showed that the impact of SST over the Sea of Japan on precipitation on the Sea of Japan side was strongly timescale-dependent. On the shorter intraseasonal timescales of several days to a few weeks, SST had a clear impact on precipitation, while the impact was indistinct when the 15-day and monthly averaged precipitation and SST values were used. On the other hand, cold surges over the Sea of Japan primarily accounted for the amount of precipitation on the Sea of Japan side. The timing and strength of cold surges controlled precipitation on all timescales. We clearly found the impact of cold surges on SST on 15-day mean values, compared with the pentad mean values. To understand detailed impacts of SST on precipitation, including air–sea interaction processes over the Sea of Japan, synoptic and shorter intraseasonal timescales should be examined in addition to seasonal or interannual timescales.

Keywords SST; precipitation; Sea of Japan; Sea of Japan side

1. Introduction

Northwesterly cold surges from the Siberian High to the Japanese archipelago result in considerable snowfall on the Sea of Japan side of Honshu (main island of Japan; see Fig. 1), Japan, in winter. The cold and dry winter monsoon from the Eurasian Continent is warmed and moistened through air-mass modification processes over the warm surface of the Sea of Japan, which is a primary source of water vapor for precipitation on the Sea of Japan side (e.g., Manabe 1957, 1958).

Hirose and Fukudome (2006) showed that the flow of the Tsushima Warm Current in autumn into the Sea of Japan, which was directly observed by ferries across the Tsushima Straits, is positively correlated with winter precipitation on the Sea of Japan side on a monthly timescale. However, their study failed to predict one of the heaviest recent snowfall events,

Corresponding author: Hiroshi G. Takahashi, Graduate School of Urban Environmental Sciences, Tokyo Metropolitan University, and Japan Agency for Marine-Earth Science and Technology, 1-1 Minami-Osawa, Hachioji, Tokyo, 192-0397, Japan
E-mail: hiroshi3@tmu.ac.jp

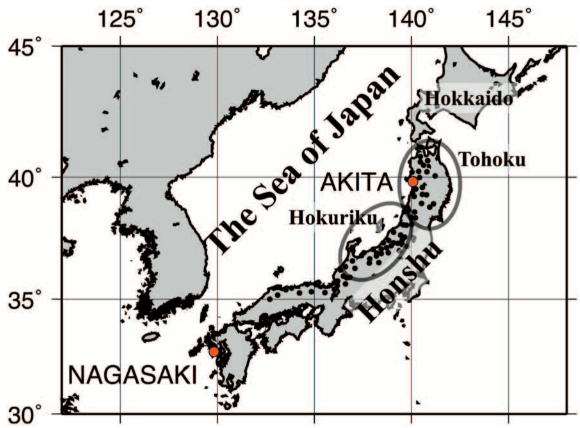

Fig. 1. Study area and observation points: black circles, AMeDAS stations; red circles, meteorological stations at Nagasaki and Akita.

which occurred in winter 2005–2006. Takano et al. (2008) reported that an anomalous atmospheric circulation pattern primarily accounted for the heavy snowfall event on the Sea of Japan side in December 2005. In addition, they showed that higher sea surface temperatures (SSTs) during late autumn over the Sea of Japan are associated with the enhanced air-mass modification on the interannual timescales. Yamamoto and Hirose (2008, 2009) conducted mesoscale model experiments and prescribed realistic SSTs produced by an oceanic general circulation model assimilated with observational data. They indicated that SSTs are significant in the simulation of realistic atmospheric circulation over the Sea of Japan and precipitation on the Sea of Japan side. Takahashi et al. (2013) used a high-resolution regional climate model to show that 1-K SST warming resulted in approximately 10% increase in precipitation over the Sea of Japan. Moreover, Yamamoto and Hirose (2011) suggested the impact of SST over the Sea of Japan on large-scale Asian monsoon circulation in winter via active cyclogenesis. Thus, it is quite possible that high SSTs over the Sea of Japan contributes to the considerable precipitation and snowfall on the Sea of Japan side in winter, although observational studies have failed to show a positive correlation between these two phenomena. In fact, Matsumura and Xie (1998) observed lower SSTs over the Sea of Japan during stronger winter monsoon years than those occurring during weaker monsoon years, which can be attributed to air-mass modification by stronger winter monsoons.

The latent heat flux from the sea surface is known to be controlled by the difference between the saturated water vapor pressure of SST and near-surface water vapor pressure in addition to the surface wind speed over the sea. Hence, higher SSTs and stronger winds are two major factors increasing the latent heat flux from the sea surface. However, SSTs decrease as a result of latent and sensible heat fluxes supplied from the sea to the atmosphere, which obscure the impact of SST on the latent and sensible heat fluxes, and in turn, on precipitation. Thus, air–sea interactions must be considered to understand the cause–effect relationship between SST and precipitation/snowfall changes. Moreover, because SST changes occur not only on seasonal and interannual timescales but also on timescales shorter than a month, the relationship between SST and precipitation must also be examined on timescales shorter than a month.

This study examined the effect of SST over the Sea of Japan on precipitation and snowfall on the Sea of Japan side of Honshu by using observational datasets and focusing on air–sea interactions on shorter intraseasonal timescales of several days to a few weeks. Moreover, we developed a cold surge index for the Asian winter monsoon to evaluate its strength on the shorter timescales. We expect that this study will contribute to the understanding of air–sea interactions over the Sea of Japan.

The remainder of this paper is organized as follows. Section 2 documents the data used in this study, and Section 3 presents an investigation of the passive and active effects of SST on precipitation and snowfall. Possible explanations for the masked impact of SST on precipitation are discussed in Section 4, and conclusions are given in Section 5.

2. Data and winter monsoon index (WMI)

To investigate the precipitation amount on the Sea of Japan side of Honshu associated with SST changes over the Sea of Japan, we used daily precipitation and snowfall observed at 76 Automated Meteorological Data Acquisition System (AMeDAS) stations (locations in Fig. 1) of the Japan Meteorological Agency. These stations have continuously observed precipitation and snowfall during 25 winters from 1982–1983 to 2006–2007. Here daily snowfall is defined as the 24-h accumulation of new snow on the basis of an hourly increase in snow depth. Because the daily snowfall data do not consider differences and temporal changes in snow density, comparing this daily snowfall accumulation with maximum snow depth or snow water equivalent values may be difficult. To create an index of broad-scale variations in precipitation and snowfall, we averaged the precipitation and snowfall amounts at all 76 stations only on Honshu, which we refer to as PRECIP and SNOW, respectively. This location was chosen because preliminary results indicated that the regional characteristics of precipitation and snowfall variations on Hokkaido (see Fig. 1) differed from those on Honshu.

To investigate interannual variations in SST associated with precipitation and snowfall on the Sea of Japan side of Honshu, we used the Centennial *in situ* Observation Based Estimates SST (COBE-SST; Ishii et al. 2005). This global monthly dataset has a spatial resolution of 1°. For variations in the shorter timescales, we also used the global high-resolution Optimum Interpolation SST (OISST; Reynolds et al. 2007) Version 2 dataset, which has a spatial resolution of 0.25° and daily temporal resolution. To create an index of SST over the Sea of Japan, we averaged the OISST values on the windward side of Honshu (130°E–138°E, 37°N–40°N). Because the spatial and temporal variations in SST over the Sea of Japan may depend on the algorithm used to calculate SST, we used two additional monthly SST datasets, the Hadley Centre sea–Ice and SST V1.1 (HadISST; Rayner et al. 2003) and extended reconstructed SST V3 (ERSST; Smith et al. 2008) datasets (Appendix B), having a spatial resolution of 1° and 2°, respectively.

To characterize the cold surge activity of the Asian winter monsoon on the shorter intraseasonal timescales, we defined the new WMI as the difference in sea level pressure between the Akita and Nagasaki meteorological stations (Fig. 1). This difference is proportional to the pressure gradient force over the Sea of Japan side of Honshu. We defined a "cold surge" as that occurring when WMI continuously exceeded 5.22 hPa for more than two days, where 5.22 hPa is the average WMI value during the 25 winters. A simple calculation shows that the geostrophic wind is approximately 5 m s^{-1} when WMI is 5.22 hPa. We confirmed that WMI defined in this way can capture cold surges of the Asian winter monsoon over the Sea of Japan on both synoptic and shorter intraseasonal timescales.

In addition, we used daily mean horizontal winds at 850 hPa and sea surface pressure, from the JRA25 (JRA25; Onogi et al. 2007) data, to examine the representation of cold surge by WMI.

3. Results

3.1 Cold surges over the Sea of Japan

We first investigated the accuracy of the representation of cold surge events by WMI because precipitation and snowfall variations are generally associated with cold surges of the Asian winter monsoon. Previously, the monsoon index (MOI), defined as the difference of sea level pressure between Irkutsk (Russia) and Nemuro (Hokkaido, Japan) was used as an index of the Asian winter monsoon. However, our preliminary study showed that MOI did not correspond to the winter monsoon activity on the shorter timescales or the cold surges of the Asian winter monsoon near Honshu, Japan (Appendix A). We prepared a composite map of the pentad mean wind field at 850 hPa over the Japanese archipelago (Fig. 2). We defined an active surge pentad as one during which the mean WMI value exceeded one standard deviation from the mean pentad WMI value. The climatological 850-hPa winds over the Sea of Japan are strong northwesterlies. The spatial pattern of difference between the composite and climatological 850-hPa wind fields shows anomalous northwesterlies over the Sea of Japan associated with an anomalous cyclonic circulation over east Hokkaido Island, which enhance the climatological mean winter monsoon (Fig. 2b). These enhanced northwesterlies over the Sea of Japan are very likely to be the typical cold surges of the Asian winter monsoon. Interestingly, the equatorward northerlies were also enhanced near Taiwan (Fig. 2b), which may be associated with the modulation of equatorial convective systems (e.g., Chang et al. 2003; Takahashi et al. 2011). These results suggest that WMI can capture the large-scale cold surges that particularly affect the Sea of Japan side of Honshu. We also compared the activity of the Asian winter monsoon on the shorter timescales between WMI and JRA25. We simply defined the strength of the Asian winter monsoon in JRA25 as the 850-hPa wind velocity $\sqrt{u^2 + v^2}$ at 135°E, 37.5°N over the Sea of Japan. The variation on the pentad mean timescale of the Asian winter monsoon indicated by WMI clearly corresponds to that by JRA25 (Fig. 3). Note that clear differences in the strength of the Asian winter monsoon among the months were not observed. In addition, our examination of many cold surge events showed that WMI can capture cold surges on the shorter intraseasonal timescales.

We examined the relationship of WMI with PRECIP and SNOW in December, January, and February on various timescales including pentad, 10-day, 15-day, and 30-day means and detected strong correlations among them (Table 1). These results support the empirical observational fact that cold surges over the Sea of Japan coincide with increased precipitation on the Sea of Japan side. With PRECIP,

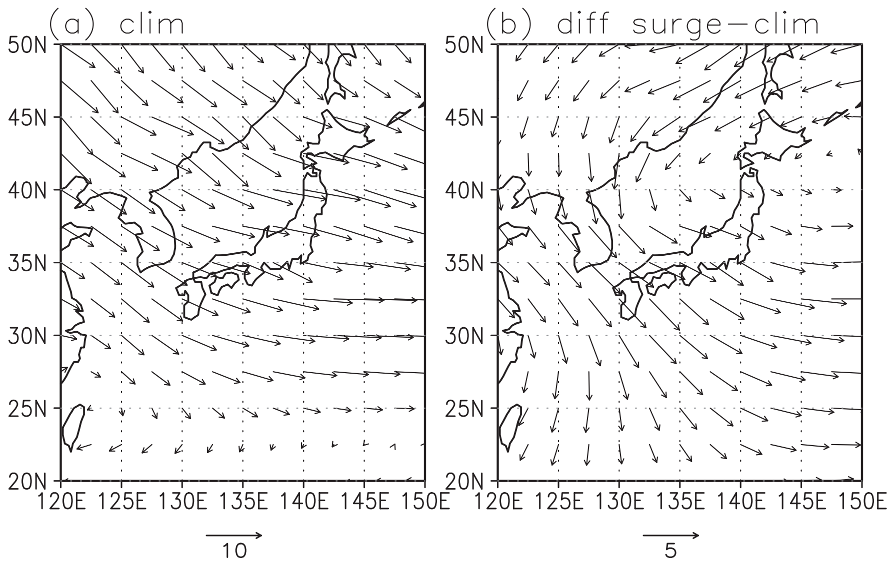

Fig. 2. (a) Composite map of 850-hPa winds over 25 winters. (b) Difference between the climatology and composite of the active surge pentads. Active cold surge pentads are those during which the mean WMI value exceeded one standard deviation from the mean pentad WMI value. The sample number of pentad for the composite is 74. Units are m s^{-1}.

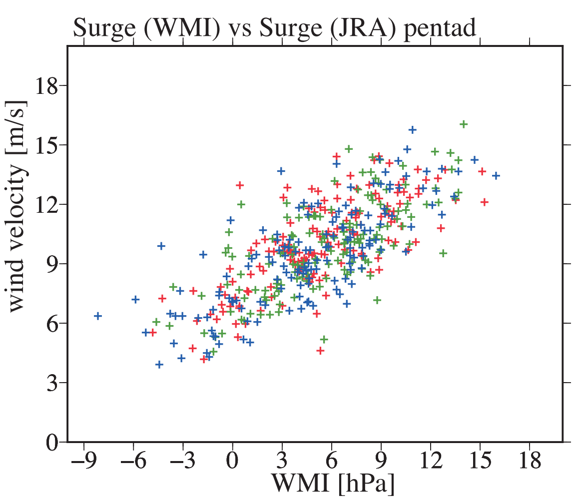

Fig. 3. Scatter plot between pentad mean WMI and the pentad mean strength of the Asian winter monsoon defined by wind velocity at 850 hPa over the Sea of Japan (JRA25). Red, green, and blue show data for December, January, and February, respectively. In order for each month to have the same number of days (30 for each), the days in each month were assigned as follows: for December: December 1–30; for January: December 31 through January 29; and for February: January 30 through February 28.

higher correlations were observed in December, although small differences were noted among the months. On the other hand, lower correlations between WMI and SNOW were detected in December, which can be associated with the sub-seasonal progression of surface air temperature. These results indicate that cold surges are necessary for the occurrence of precipitation during the entire winter. Finally, we quantitatively examined the relationships between the WMI and PRECIP on a pentad mean timescale and for individual events. On the pentad mean timescale, stronger cold surges, indicated by higher WMI values, were associated with larger amounts of precipitation on the Sea of Japan side (Fig. 4). In contrast, the relationship for individual cold surge events, although positive, was slightly weaker than that for the pentad mean timescale, which suggests that the relationship is not likely to be monotonic or linear. In particular, when WMI was higher than 12 hPa, the amount of precipitation increase became unclear.

3.2 *Impact of SST on precipitation on various timescales*

Next, we investigated the association of SSTs over the Sea of Japan and PRECIP. Interannual variations in PRECIP in the northern winter (December–February; DJF) and in the individual months of December, January, and February are shown in Fig. 5. The 25-

Table 1. Correlation coefficients between the WMI and precipitation or accumulated snowfall over 25 years during winter months of December, January, and February on various timescales including pentad, 10-day, 15-day, and 30-day means. Here December is from December 1 to 30, January is from December 31 to January 29, and February is from January 30 to February 28.

	precipitation			snow		
	Dec	Jan	Feb	Dec	Jan	Feb
Pentad	0.77	0.66	0.68	0.62	0.72	0.76
10-day	0.77	0.72	0.62	0.57	0.77	0.77
15-day	0.73	0.69	0.61	0.50	0.80	0.78
30-day	0.76	0.73	0.74	0.60	0.80	0.74

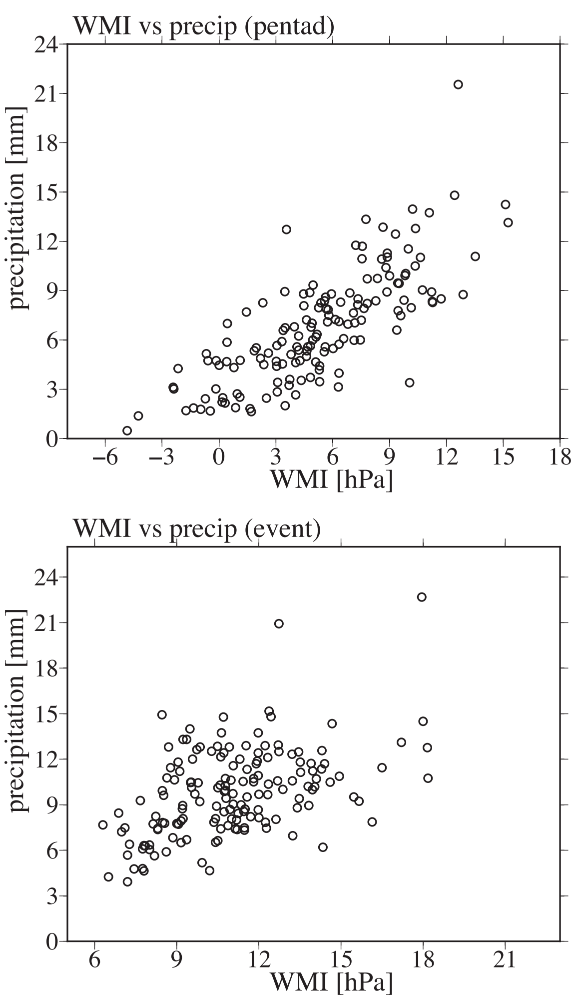

Fig. 4. Scatter diagrams between pentad mean WMI and pentad mean PRECIP (top) and between mean WMI and PRECIP during cold surge events (bottom). The cold surges lasted from 1 to 28 days.

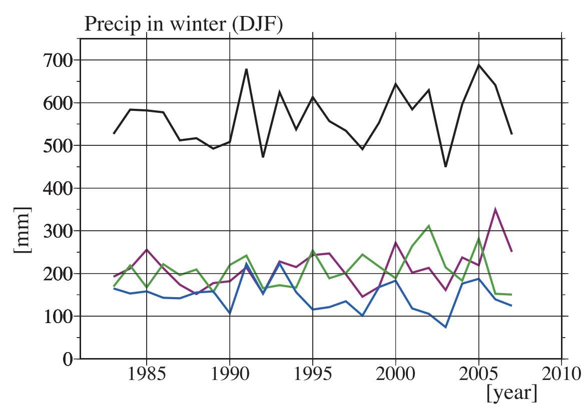

Fig. 5. Interannual variation in total precipitation in winter (December, January, and February; DJF; black) and in individual months of December (purple), January (green), and February (blue) from 1984 to 2007.

year mean PRECIP in DJF was 564.8 mm, and its interannual standard deviation was 62.8 mm. The range of interannual variation in PRECIP, defined as one standard deviation, was approximately 11% of the total precipitation.

We then chose the four highest and lowest PRECIP years for DJF among the 25 years, as well as the four highest and lowest PRECIP years separately for December, January, and February, to prepare composite maps of SST differences between high and low PRECIP years (Fig. 6). In addition, we conducted similar composite analyses by using the other three SST datasets; these results are shown in Appendix B. For DJF as a whole, no clear signal was found over the Sea of Japan; however, a low SST anomaly was observed over the East China Sea, and a high SST anomaly was detected near Hokkaido. In December, a low SST anomaly was observed over the East China

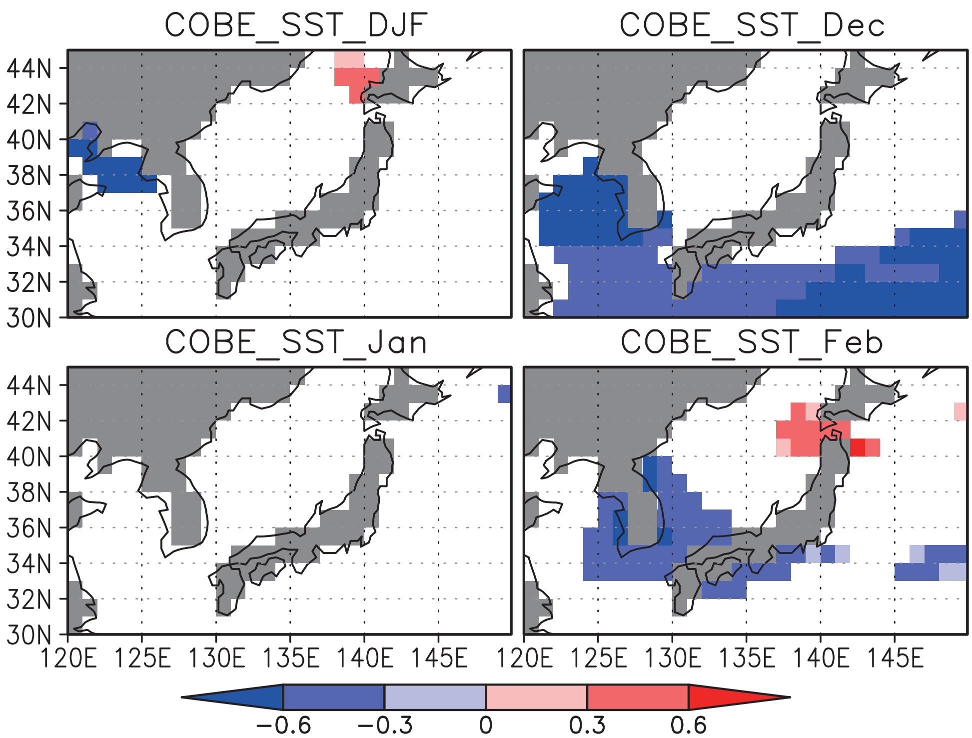

Fig. 6. Spatial patterns of composite COBE-SST anomalies between years of high and low average precipitation of 76 stations on Honshu (PRECIP) in (a) DJF, (b) December, (c) January, and (d) February. The four highest and lowest PRECIP years were used. SST anomalies with a local significance level of 90% are plotted, as determined using Student's t-test.

Sea. However, no statistically significant SST anomaly was observed over the Sea of Japan in December or January. In February, a low SST anomaly was found over the western Sea of Japan, and a high SST anomaly was observed near the Tohoku District. The SST signals observed in February were essentially common among the four SST datasets, whereas the SST signals in DJF, December, and January were more widespread (Appendix B, Figs. B1–3). These results suggest that the negative relationship between precipitation on the Sea of Japan side and SST over the Sea of Japan in February was relatively robust, although the other signals observed in December and January may depend on the particular datasets. Therefore, considerable precipitation on the Sea of Japan side is not associated with simultaneous SST anomalies over the Sea of Japan on monthly and seasonal timescales. The negative relationship between SST over the Sea of Japan and precipitation on the Sea of Japan side of Honshu is consistent with the findings of a previous study (Matsumura and Xie 1998). On a monthly timescale, the increased precipitation due to warmer SSTs may be obscured by the effect of the decline in SST as a result of the cold surge activity. However, no previous study has investigated the relationship between SST over the Sea of Japan and precipitation on the Sea of Japan side of Honshu on the shorter timescales.

Therefore, to determine such an association, we examined the impact of SST for individual events, and pentad, 15-day, and 30-day mean timescales. As previously reported, SST can be modified by a cold surge activity via air-mass modification, which can mask the impact of SST on precipitation. To avoid this effect, we compared the pentad mean SST just prior to a cold surge event with precipitation during the event and that during pentad, 15-day, and 30-day periods. In addition, to avoid duplicity, we used only events separated by more than five days. Figure 7 shows the interannual variations in monthly mean SST in November, December, January, and February over the Sea of Japan, which indicates a gradual decrease with the seasonal wintertime progression. For each month, SST varied interannually by approximately 2°C, whereas the monthly sub-seasonal changes in SST in winter were 2–3°C. Because such sub-seasonal progression of SST is comparable to interannual SST variation, we plotted the symbols for each month in Fig. 8 to distinguish these factors.

Figure 8 shows the respective impacts of SST and cold surges of the winter monsoon on precipitation. In our analysis of individual events, we found that the amount of precipitation increased with SST. On the pentad mean timescale, precipitation clearly increased with SST when WMI was 5–12 hPa. Moreover, increases in precipitation with SST were clear within each month, which suggests that warmer SSTs over the Sea of Japan cause higher precipitation amounts on the Sea of Japan side. When WMI was higher than 12 hPa, the impact of SST on precipitation became unclear, which indicates that very strong cold surges can reduce or cancel the influence of SST. In addition, several high precipitation events were detected when WMI was lower than approximately 6 hPa. Examination of such events in the pentad timescale under such low WMI conditions revealed that short-lived cyclonic disturbances over the Sea of Japan were associated with several instances of increased precipitation. However, although most of these disturbances did not increase PRECIP on the Sea of Japan side of Japan, they may increase precipitation on local or regional scales. Thus, cold surges of the winter monsoon are major factors that increase PRECIP on the pentad timescale.

Note that the impact of SST from the pentad mean values was clearer in December than those in January and February. Moreover, the range of interannual variation in SST was the largest in December and smallest in February. This sub-seasonal difference in impact of SST on precipitation will be discussed in Section 4.2.

Note that the cold surge activity is an important factor in the increase in precipitation. Because SST generally declines with sub-seasonal progression from November to February, higher SST events often occurred in December, and lower SST events were observed in February. On the 15-day mean timescale, SST did not show a clear impact on precipitation, although strong cold surges were associated with increased precipitation. On the 30-day mean timescale, the impact of cold surges on precipitation was very clear, but that of SST was unclear. These results suggest that the impact of SST is distinct only on the shorter intraseasonal timescales, while that of cold surges is very clear on all timescales. We discuss a possible explanation for timescale dependency of SST impact on precipitation in Section 4.1.

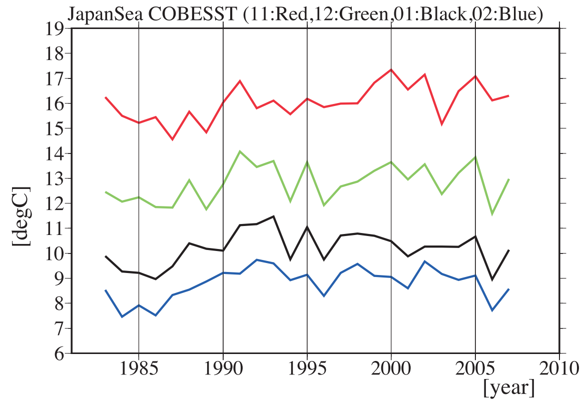

Fig. 7. Interannual variation in SST over the Sea of Japan in November (red), December (green), January (black), and February (blue).

We also investigated SST impact on snowfall (Fig. 9) for pentad and 15-day averages. An increased amount of SNOW was associated with active cold surges, whereas the SST impact on the amount of SNOW was unclear. In addition, a sub-seasonal difference in the amount of SNOW was clearly observed, which is probably associated with the sub-seasonal progression of proportion of rainfall amount to total precipitation due to that of surface air temperature from December to February. In particular, in December, most precipitation was observed as rainfall, which was responsible for warm surface air temperatures. In addition, sub-seasonal progression of snowfall density may be associated with the sub-seasonal difference in the amount of SNOW. This result is likely associated with the lower correlation coefficient between WMI and SNOW in December, compared with that in January and February (Table 1). Thus, a cold surge associated with high SST conditions does not always correspond to a heavy snowfall event.

To reconfirm the impact of SST on PRECIP and understand the spatial scale of effective SST anomalies over the Sea of Japan, we investigated the relationship between pentad mean precipitation and SST just prior to the pentad (Fig. 10). As shown in Fig. 8, the impact of SST on precipitation was clear when WMI was 5–12 hPa. Therefore, to reveal the effective SST anomalies for the increases in PRECIP, we calculated the correlation coefficient between pentad mean PRECIP and SST just prior to the pentad on each grid only when WMI was 5.22–12 hPa. A statistically significant positive correlation was detected over and near the

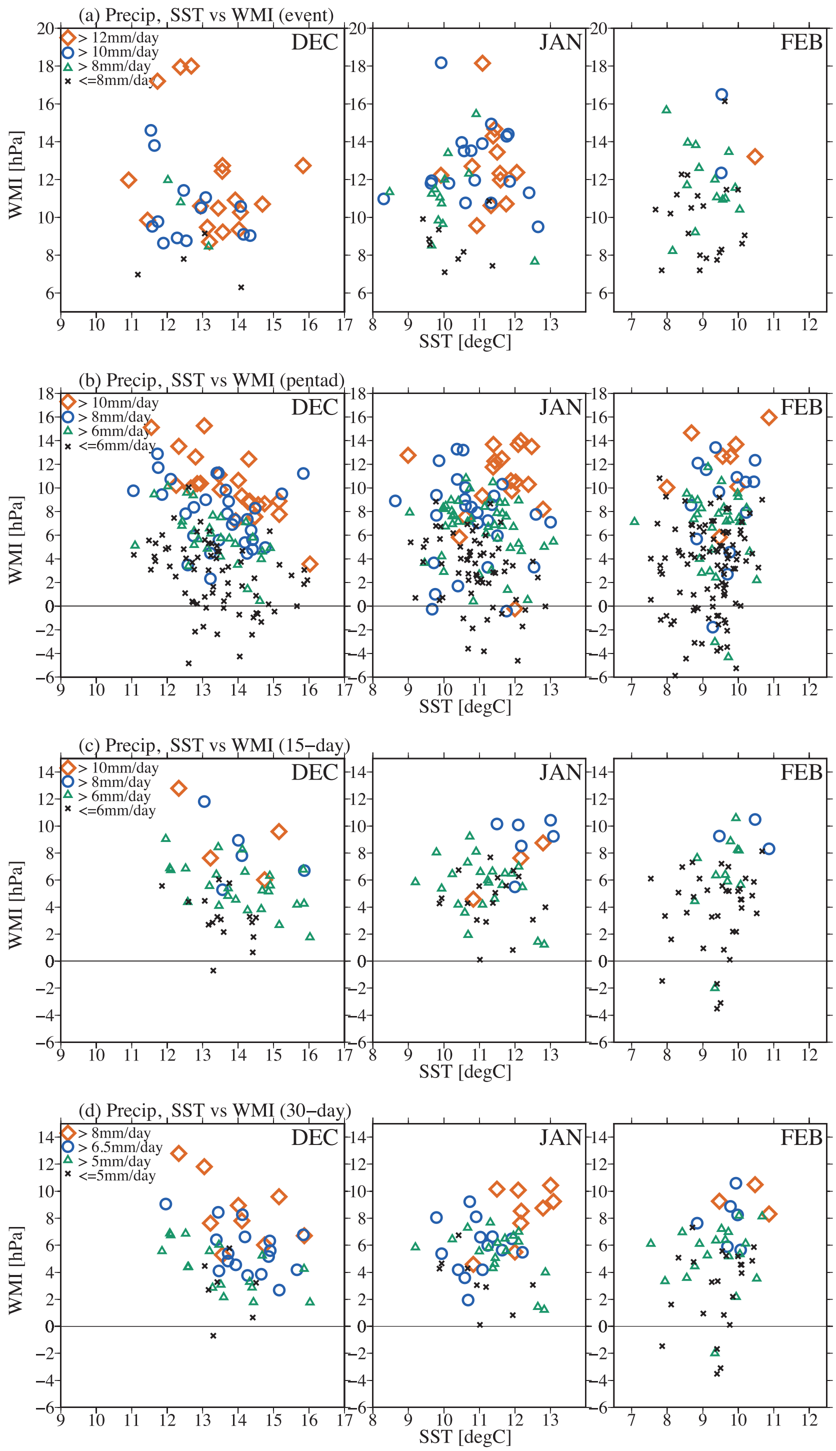

Fig. 8. Scatter diagrams indicating differences between SST and WMI on an (a) event scale and timescales of (b) pentad, (c) 15 days, and (d) 30 days. The symbols of precipitation amount indicate at the upper left of the left (December) panel. Here December is from December 1 to 30, January is from December 31 to January 29, and February is from January 30 to February 28.

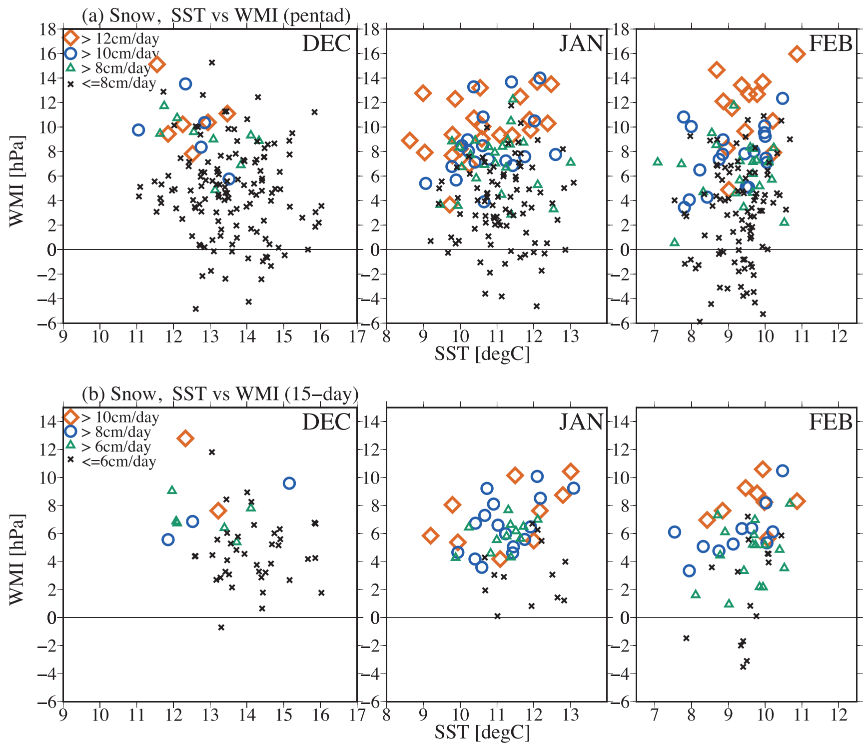

Fig. 9. Scatter diagrams indicating differences between SST and WMI for timescales of (a) pentad and (b) 15 days. The symbols of the daily accumulated snowfall amount indicate at the upper left of the left (December) panel. Here December is from December 1 to 30, January is from December 31 to January 29, and February is from January 30 to February 28.

reference region in December and January. Positive correlations were observed over and around the reference region in February, although the signals were not significant at the 95% confidence limit. This result implies that warmer SSTs over the Sea of Japan cause higher precipitation amounts on the Sea of Japan side of Japan. Note that significant SST anomalies were observed not only near the coast of Japan but also in a broader area of the Sea of Japan, including the reference region. The various degrees of SST impact on precipitation in December, January, and February are discussed in Section 4.2. The regional differences of impact of SST and cold surges should be investigated in a future study.

3.3 SST declines due to cold surges

Finally, we investigated the impact of cold surges of the Asian winter monsoon on SST. As described in Section 3.2, we found that precipitation on the Sea of Japan side of Honshu was either negatively or not correlated with SST interannual anomalies, a result that was probably related to a decline in SST caused by cold surges. We, therefore, examined the decline in SST associated with the cold surges of the Asian winter monsoon by plotting changes in SST during 15-day periods against the WMI and 15-day mean precipitations against changes in SST during the 15-day periods (Figs. 11a and 11b).

We found that the changes in SST are negatively correlated with WMI and that this negative relationship is more evident when the data for each month are examined separately (Fig. 11a). This result may be attributed to the sub-seasonal winter progression of SST and that of surface air temperature because the sub-seasonal differences in the cold surge activity were small (Fig. 3). This negative relationship is consistent with the result of Matsumura and Xie (1998) and can be explained by larger latent and sensible heat fluxes from the ocean to the atmosphere. Note that the impact of cold surges on SST was found on 15-day averaged values, which implies that the timescale of atmospheric impact on SST is also much shorter than one month. Other factors, such as interannual variations in SST and ocean currents, can modulate the relationship. In

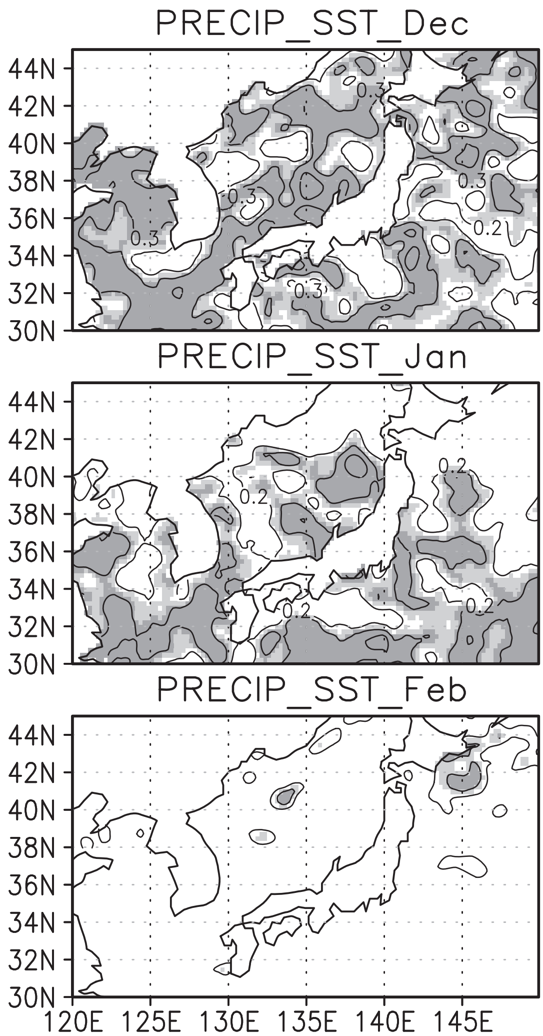

Fig. 10. Spatial maps of correlation coefficients between the pentad mean PRECIP and SST just prior to the pentad at each grid. We calculated the correlation, only when WMI was from 5.22 hPa to 12 hPa. Dark (light) gray shading denotes statistical significance at the 95% (90%) confidence limit. Here December is from December 1 to 30, January is from December 31 to January 29, and February is from January 30 to February 28.

addition, on the 15-day mean timescale, the decline in SST over the Sea of Japan clearly correlated with the 15-day mean precipitation on the Sea of Japan side (Fig. 11b). Because the moisture content of the cold air mass is very low over Eurasia, most of the water vapor is supplied from the Sea of Japan. The amount of water vapor supplied to the air mass strongly depends on the decline in SST, which can explain the strong negative relationship between SST and PRECIP. Similar results were obtained on the 30-day mean timescale (not shown).

To understand the timescale of impact of cold surges on SST, we also created scatter plots between WMI and SST changes (Fig. 11c) and between changes in SST and PRECIP (Fig. 11d) on the pentad timescale. The correlation between WMI and changes in SST on the pentad timescale was weaker than that on the 15-day timescale (Table 2). In addition, changes in SST weakly correlated with PRECIP on the pentad timescale. This result suggests that the impact of atmospheric circulation on SST is unclear on the pentad timescale. Therefore, the effective timescale of atmospheric impact on SST is probably longer than 5 days but shorter than 15 days. Hence, as shown in Figs. 8, 9, and 11, the interaction between SST and atmosphere is clear on the shorter intraseasonal timescales.

4. Discussion

4.1 Timescale dependency of air–sea interactions over the Sea of Japan

SST over the Sea of Japan should affect precipitation on the Sea of Japan side of Honshu, but this effect has not been shown by observational data analysis, probably because of the timescale of air–sea interactions over the Sea of Japan. In this study, the impact of SST on precipitation was evident only on the synoptic and shorter intraseasonal timescales. The impact of cold surges of the Asian winter monsoon on SST was also observed on the shorter intraseasonal timescales.

The shorter intraseasonal timescales likely correspond to the timescales of water convection and diffusion processes in the ocean mixed layer. In general, although SST decreases as a result of positive latent and sensible heat fluxes from the ocean to the atmosphere, it should also gradually decrease as the overall water temperature of the mixed layer decreases. Because such heat fluxes decrease the water temperature in the entire mixed layer, the atmospheric impact on SST should be slower than that from SST to the atmosphere. However, the results showed that the atmospheric impact on SST can be observed from 15-day averaged values, which suggests the importance of air–sea interactions on the shorter intraseasonal timescales. Heat transport from the ocean to the atmosphere should be qualitatively and quantitatively examined further in future studies.

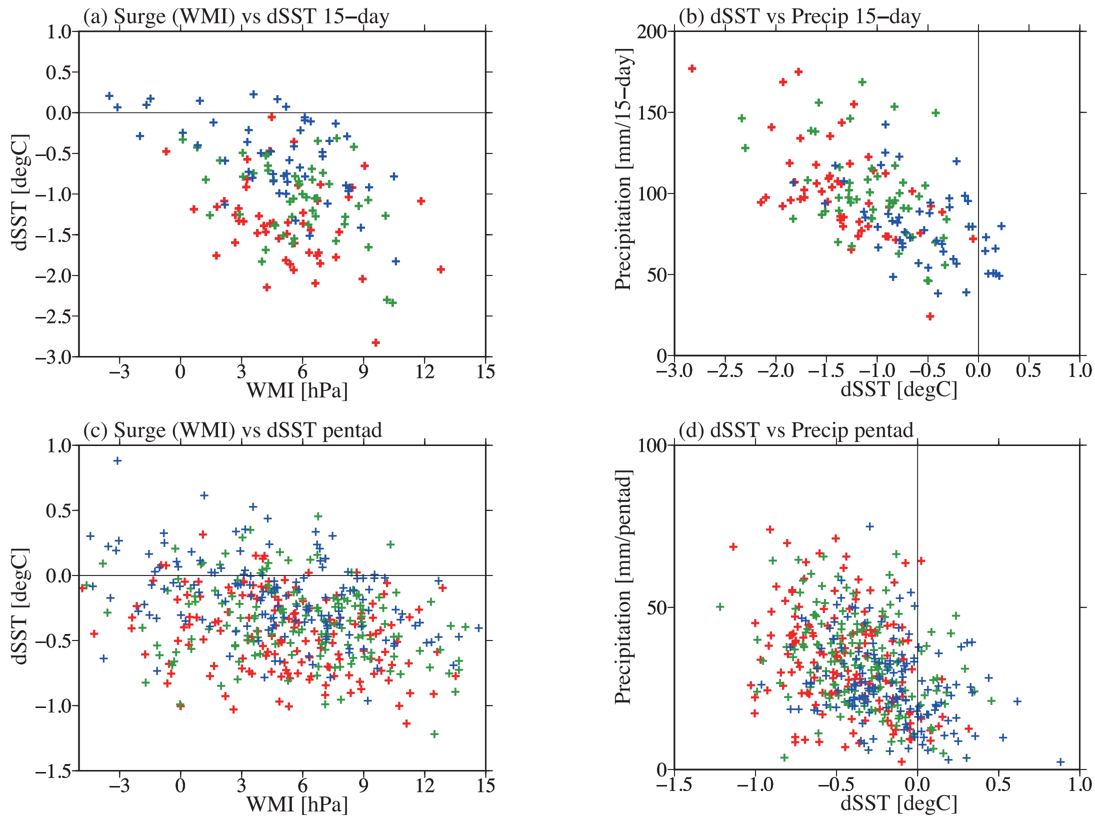

Fig. 11. Scatter plots (a) between the 15-day mean WMI and changes in SST (dSST), (b) between the 15-day mean dSST and precipitation, (c) between the pentad mean WMI and dSST, and (d) between the pentad mean dSST and precipitation. We used the OISST high dataset for SST. dSST is defined as the pentad mean SST for the last 5 days within a 15-day period ((a) and (b)) or a pentad period ((c) and (d)) minus the pentad mean SST just prior to the 15-day period or the pentad over the Sea of Japan (130°E–138°E, 37°N–40°N). The units of WMI, dSST, and precipitation are hPa, C per day, and mm per 15 days or pentad, respectively. Red, green, and blue symbols indicate December, January, and February, respectively, where December is from December 1 to 30, January is from December 31 to January 29, and February is from January 30 to February 28.

Table 2. Correlation coefficients between dSST and PRECIP or WMI over 25 years during winter months of December, January, and February on timescales of pentad and 15-day means. Here December is from December 1 to 30, January is from December 31 to January 29, and February is from January 30 to February 28. All values were statistically significant at the 95% confidence limit.

	dSST vs PRECIP		dSST vs WMI	
	pentad	15-day	pentad	15-day
Dec	0.33	0.57	0.29	0.30
Jan	0.40	0.44	0.31	0.42
Feb	0.30	0.49	0.34	0.56

4.2 Sub-seasonal difference in SST impact on precipitation on the Sea of Japan side of Japan

The impact of SST on precipitation varied among December, January, and February. As shown in Fig. 11, this impact was clearer and statistically significant in December and January than that in February. The same tendency is shown in Fig. 8. In this subsection, we discuss the sub-seasonal difference in the impact of SST on precipitation on the Sea of Japan side of Japan.

The absolute range of interannual variations in SST over the Sea of Japan in December was larger than those in the other months, which implies that SSTs in this region were more easily affected by the cold surge activity in December; therefore, the range of absolute changes in sea surface fluxes due to the SST changes was also larger than those in the other months. These sub-seasonal differences in the range of interannual SST variations are likely associated with the depth of the mixed layer of the ocean. The gradual accumulation of sea surface fluxes over the Sea of Japan is consistent with the deepening of the mixed layer of the Sea of Japan with the sub-seasonal progression from the northern fall to spring. The mixed layer of the Sea of Japan in February was deeper than that in December. Because a shallower mixed layer is easily declined by the smaller amount of exchanges of sea surface fluxes, the range of interannual SST variations in December is larger than that in the other two winter months.

In addition, the absolute changes in latent heat flux over the Sea of Japan per 1-K SST warming in December, which is the source of precipitation on the Sea of Japan side of Japan, is larger than those in the other two winter months. This is because the absolute values in SST in December were 4–5 K warmer than those in February. Because the holding capacity of water vapor in air increases by approximately 7% per 1-K warming and is governed by the Clausius–Clapeyron equation, the water vapor amount also increases by approximately 7% per K of warming under conditions of unchanged relative humidity. When wind speed and difference between surface air temperature and SST are the same, the absolute change in latent heat flux due to 1-K SST changes becomes larger in December than that in the other months. Thus, the absolute values of latent heat flux over the Sea of Japan differ significantly between December and February; other factors likely modulate precipitation and mask the impact of SST on precipitation in the latter month.

4.3 Masked positive impact of SST on precipitation

A positive simultaneous correlation was not observed between SST and precipitation because the cold surge activity is necessary for precipitation to occur. Let us consider two cases with the same initial SST conditions. In the first case, atmospheric conditions indicate an active winter monsoon with one or more cold surges, while in the second case, no cold surge occurs. A comparison of monthly mean SSTs with and without a cold surge shows that SST in months without a cold surge is higher because cold surges decrease SST over the Sea of Japan. For this reason, a positive interannual correlation between SST and precipitation is not apparent on a monthly or longer timescale.

This study also examined the impact of the pentad mean SST on precipitation just prior to a cold surge event during the event and during pentad, 15-day, and 30-day periods. We found the impact of SST on precipitation on the synoptic and shorter intraseasonal timescales, but not on the monthly or longer timescales. This observational fact can be mainly explained by the following two factors. 1) The memory of SSTs over the Sea of Japan can be dissipated by a single cold surge of the Asian winter monsoon. The magnitude of SST decrease in one month was comparable to that of the decrease that occurs during a single cold surge event. 2) Cold surge activity can differ slightly, even when the monthly mean WMI is the same. Hence, these effects can obscure the impact of SST on precipitation on the monthly timescale.

5. Conclusions

Focusing on synoptic and shorter intraseasonal timescales, this study examined the impact of SST on precipitation on the Sea of Japan side of Honshu during 25 winters from 1982–1983 to 2006–2007 by using four SST datasets, JRA25 data, and surface observations of precipitation.

We developed WMI, which represents the cold surge activity of the Asian winter monsoon on the various timescales. Because SSTs are reduced by the cold surge activity, we used a pentad mean SST just prior to a cold surge event and during pentad, 15-day, and 30-day periods. The results showed that on intraseasonal timescales shorter than a 15-day mean period, higher SSTs over the Sea of Japan led to a larger amount of precipitation on the Sea of Japan side of Honshu in winter. High SST events often occurred more frequently in December and low SST events occurred more frequently in February because of the seasonally decreasing progression of SST. Note that the impact of SST on precipitation was unclear on the monthly mean timescale. In addition, the impact of SST on snowfall was more complicated because the proportion of rainfall amount to total precipitation varies over the course of the winter with the sub-seasonal progression of surface air temperature. Therefore, a heavy snowfall event does not always accompany a cold surge event with high SST. Nevertheless, the SST effect on precipitation and snowfall was of secondary importance. The impact of winter monsoon cold surges on large amounts of rainfall and snowfall on the Sea of Japan side of Honshu was primarily significant on timescales from synoptic to seasonal.

The impact of cold surges on SST over the Sea of Japan was observed on a timescale of a few weeks but

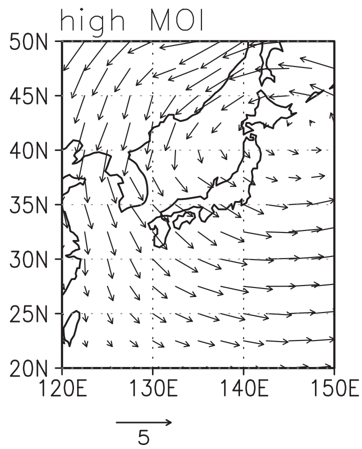

Fig. A1. Difference between the climatology and composite of the active surge pentads of MOI. Active surge pentads during which the MOI value exceeded one standard deviation from the mean pentad MOI value. The sample number of pentad is 74. Units are m s^{-1}.

Table A1. Correlation coefficients between WMI or MOI and PRECIP on the daily, 3-day, pentad, 15-day, 30-day, and seasonal (90-day) mean timescales over 25 winters from 1982–1983 to 2006–2007.

	WMI	MOI
daily	0.67	0.46
3-day	0.69	0.50
pentad	0.69	0.53
15-day	0.63	0.54
30-day	0.62	0.54
90-day	0.57	0.61

not on the pentad timescale, which indicates a shorter intraseasonal timescale for atmospheric impact on SST. However, the timescale of the atmospheric impact was longer than that from SST to the atmosphere. Hence, investigations of air–sea interactions on the shorter intraseasonal timescale are needed, to determine the detailed effects of SST on precipitation on the Sea of Japan side of Japan.

The impact of SST on precipitation on the Sea of Japan side of Japan in December was more pronounced than that in February. This result can be explained by the sub-seasonal progression of the depth of the mixed layer and absolute differences in latent heat flux associated with the absoute values of SSTs.

When we compared changes in SST during between active winter monsoon month and inactive one, monthly domain-averaged SSTs over the Sea of Japan were higher in the inactive ones, although precipitation on the Sea of Japan side was higher under the active ones. These results are consistent with the fact that simultaneous relationships between SST and WMI were negative on 15- and 30-day mean timescales. It is highly likely that the impact of SST on precipitation is obscured on the monthly timescale, although this effect is significant during individual cold surge events. Thus, further investigations of the impact of SST on precipitation with consideration of the quantitative effects of air–sea interactions are necessary.

Acknowledgments

NOAA High Resolution SST data was provided by the NOAA/OAR/ESRL PSD, Boulder, Colorado, USA, from their Web site at http://www.esrl.noaa.gov/psd. We are grateful to Dr. Yoshihiro Tachibana of Mie University for his positive scientific comments. We also thank an anonymous referee for useful comments. We thank Dr. Jun Matsumoto for his helpful comments. This work was partly supported by Leading Scientist Award Fund of Tokyo Metropolitan University, “Green Network of Excellence (GRENE)” program and Research Program on Climate Change Adaptation (RECCA) Fund by Ministry of Education, Culture, Sports, Science, and Technology (MEXT), Japan.

Appendix A

In this appendix, we examined the representativeness of MOI. In this study, MOI was calculated using JRA25. Nearest grids of Irkutsk and Nemuro were used for the calculation. The spatial difference in 850-hPa winds showed that enhanced northwesterlies were found over the Sea of Japan (Fig. A1), which was similar to WMI composite. However, the enhanced northwesterlies were weaker around Hokuriku and Tohoku Districts than those of WMI. We also calculated correlation coefficients between WMI or MOI and PRECIP on the basis of the daily, 3-day, pentad, 15-day, 30-day and seasonal averaged values (Table A1). We calculated WMI and MOI using JRA25, because WMI calculated from meteorological stations was basically the same as WMI calculated from JRA25. Except for Table A1, we used the WMI calculated from the observation at meteorological stations. Compared with WMI, MOI was weakly correlated to PRECIP particularly on the shorter timescales. On the other hand, MOI showed a slightly

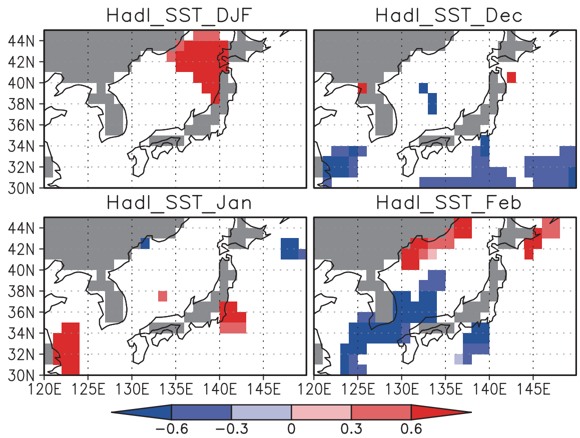

Fig. B1. Spatial patterns of composite HadISST anomalies between years of high and low average precipitation of 76 stations on Honshu (PRECIP) in (a) DJF, (b) December, (c) January, and (d) February. The four highest and lowest PRECIP years were used. SST anomalies with a local significance level of 90% are plotted, as determined using Student's t-test.

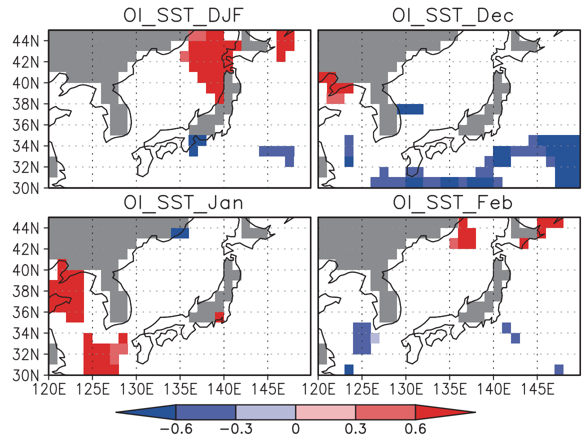

Fig. B2. Spatial patterns of composite OISST anomalies between years of high and low average precipitation of 76 stations on Honshu (PRECIP) in (a) DJF, (b) December, (c) January, and (d) February. The four highest and lowest PRECIP years were used. SST anomalies with a local significance level of 90% are plotted, as determined using Student's t-test.

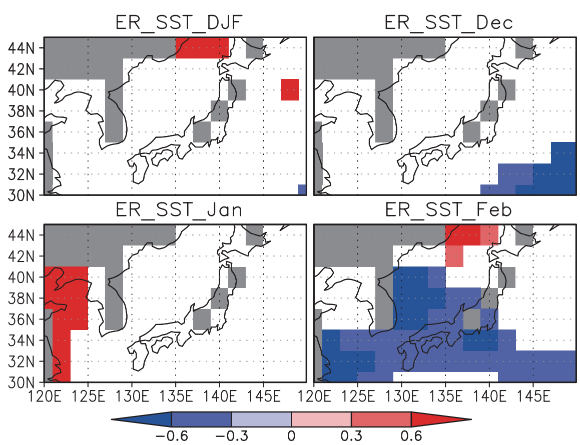

Fig. B3. Spatial patterns of composite ERSST anomalies between years of high and low average precipitation of 76 stations on Honshu (PRECIP) in (a) DJF, (b) December, (c) January, and (d) February. The four highest and lowest PRECIP years were used. SST anomalies with a local significance level of 90% are plotted, as determined using Student's t-test.

higher correlation value on the 90-day averaged values, which indicates that the MOI may be slightly better representative only on seasonal averaged interannual variations. However, the WMI was basically higher correlated with precipitation on the Sea of Japan side of Japan on various timescales. Another advantage of WMI is that the stations calculated for WMI can be modified for target regions.

Appendix B

We investigated the relationship between SST and PRECIP using multiple datasets, COBE-SST (Section 3.2), HadISST (Fig. B1), OISST (Fig. B2), and ERSST (Fig. B3).

For DJF as a whole, no clear HadISST signal was found over the central and western Sea of Japan, but a high HadISST anomaly was observed over western Hokkaido Island. In December, a low SST anomaly was observed over the central Sea of Japan, East China Sea, and south of Honshu. High SST anomalies were seen over the East China Sea and southwest of Honshu in January. In February, significantly low SST anomalies were found over the western Sea of Japan and south of Honshu, and a high SST anomaly was observed along the northern coast of the Sea of Japan. For OISST, signals of high and low SST anomalies were similar in DJF, December, and January. However, low SST anomalies over the Sea of Japan in February were not found in the OISST dataset. The patterns of the ERSST anomaly were similar to HadISST anomalies in DJF, December, January, and February.

References

Chang, C., C. Liu, and H. Kuo, 2003: Typhoon Vamei: An equatorial tropical cyclone formation. *Geophys*. *Res*. *Lett*., **30**, 1150, doi:10.1029/2002GL016365.

Hirose, N., and K. Fukudome, 2006: Monitoring the Tsushima warm current improves seasonal prediction of the regional snowfall. *SOLA*, **2**, 61–63.

Ishii, M., A. Shouji, S. Sugimoto, and T. Matsumoto, 2005: Objective analyses of sea-surface temperature and marine meteorological variables for the 20th century using ICOADS and the Kobe collection. *Int*. *J*. *Climatol*., **25**, 865–879.

Manabe, S., 1957: On the modification of air-mass over the Japan Sea when the outburst of cold air predominates. *J*. *Meteor*. *Soc*. *Japan*, **35**, 311–326.

Manabe, S., 1958: On the estimation of energy exchange between the Japan Sea and the atmosphere during winter based upon the energy budget of both the atmosphere and the sea. *J*. *Meteor*. *Soc*. *Japan*, **36**, 123–133.

Matsumura, S., and S.-P. Xie, 1998: Response of temperature and precipitation over Japan and the Japan Sea to variability of winter monsoon. *Tenki*, **45**, 781−791 (in Japanese with English abstract).

Onogi, K., J. Tsutsui, H. Koide, M. Sakamoto, S. Kobayashi, H. Hatsushika, T. Matsumoto, N. Yamazaki, H. Kamahori, K. Takahashi, S. Kadokura, K. Wada, K. Kato, R. Oyama, T. Ose, N. Mannoji, and R. Taira, 2007: The JRA-25 reanalysis. *J*. *Meteor*. *Soc*. *Japan*, **85**, 369–432.

Rayner, N., D. Parker, E. Horton, C. Folland, L. Alexander, D. Rowell, E. Kent, and A. Kaplan, 2003: Global analyses of sea surface temperature, sea ice, and night marine air temperature since the late nineteenth century. *J*. *Geophys*. *Res*., **108**, 4407, doi:10.1029/2002JD002670.

Reynolds, R., T. Smith, C. Liu, D. Chelton, K. Casey, and M. Schlax, 2007: Daily high-resolution-blended analyses for sea surface temperature. *J*. *Climate*, **20**, 5473–5496.

Smith, T., R. Reynolds, T. Peterson, and J. Lawrimore, 2008: Improvements to NOAA's historical merged land-ocean surface temperature analysis (1880-2006). *J*. *Climate*, **21**, 2283–2296.

Takahashi, H., Y. Fukutomi, and J. Matsumoto, 2011: The impact of longlasting northerly surges of the east asian winter monsoon on tropical cyclogenesis and its seasonal march. *J*. *Meteor*. *Soc*. *Japan*, **89**, 181–200.

Takahashi, H., N. Ishizaki, H. Kawase, M. Hara, T. Yoshikane, X. Ma, and F. Kimura, 2013: Potential impact of sea surface temperature on winter precipitation over the Japan Sea Side of Japan: A regional climate modeling study. *J*. *Meteor*. *Soc*. *Japan*, **91**, 471–488.

Takano, Y., Y. Tachibana, and K. Iwamoto, 2008: Influences of large-scale atmospheric circulation and local sea surface temperature on convective activity over the Sea of Japan in December. *SOLA*, **4**, 113–116.

Yamamoto, M., and N. Hirose, 2008: Influence of assimilated SST on regional atmospheric simulation: A case of a cold-air outbreak over the Japan Sea. *Atmos*. *Sci*. *Lett*., **9**, 13–17.

Yamamoto, M., and N. Hirose, 2009: Regional atmospheric simulation of monthly precipitation using high-resolution SST obtained from an ocean assimilation model: Application to the wintertime Japan Sea. *Mon*. *Wea*. *Rev*., **137**, 2164–2174.

Yamamoto, M., and N. Hirose, 2011: Possible modification of atmospheric circulation over the northwestern Pacific induced by a small semienclosed ocean. *Geophys*. *Res*. *Lett*., **38**, L03804,doi:10.1029/2010GL046214.